Image Based Smoke Detection with Two–Dimensional Local Hurst Exponent

Hidenori Maruta*, Takeshi Yamamichi†, Akihiro Nakamura†, Fujio Kurokawa*†‡
*Information Media Center, Nagasaki University
1 - 14 Bunkyo, Nagasaki-shi, Nagasaki, 852-8521 Japan
Email: hmaruta@nagasaki-u.ac.jp
†Graduate School of Science and Technology, Nagasaki University
Email: {d708104h, d709026h}@cc.nagasaki-u.ac.jp
‡Faculty of Engineering, Nagasaki University
Email: fkurokaw@nagasaki-u.ac.jp

***Abstract*—For early fire detection, smoke is considered as an important sign for it. Image based detection methods more useful than other methods which use some special sensor devices because of the cost and difficulties in setting them around target areas. When treating the image information of smoke, it is important to consider characteristics of smoke such as the semi–transparency, the non–stationary shape and so on. In this study, we use the nature of smoke and examine a smoke detection method based on a fractal nature of smoke as it is well–known that smoke is considered as fractal. We consider that the image information of smoke is a self-affine fractal. From this assumption, we can characterize the fractal nature of smoke with the exponent of fractal. We use the Hurst exponent H, which is one of the widely known exponent of fractal. We numeriacally calculate H of smoke from the relation between H and the wavelet transform of the image. So we detect the smoke area in images with H through the wavelet transform. Moreover, to obtain the accurate detection result, we use the time–accumulation technique to smoke detection results of each image. In the experiment, we examine the performance of our method based on the fractal property of smoke.**

I. Introduction

Especially in large facilities such as large ports, chemical plants and power plants, the fire largely affect the surrounding areas. In such open areas, the direct fire or flames detection methods [1], [2], [3] are sometime very limited because sources of the fire or flames cannot always fall into the field of view of sensors due to their positions and sizes. So the smoke detection is needed for the early fire detection. However, it is difficult to set special devices for sensing of smoke due to its cost, areal conditions and so on. In these cases, image based methods are useful because they can be to serve to solve these problems. In most of such areas, surveillance cameras are already set hence we can easily obtain image information of target areas using them. From these reasons, we consider to use a computer vision approach for smoke detection.

Smoke gradually grows and always exists until the source of smoke disappear. When we treats the image information of smoke, we have some difficulties mainly due to following characteristic properties of smoke such as semi–transparency, non–stationary shape, sensitiveness to environmental conditions (complex backgrounds, the direction and the velocity of the wind, etc.).

In general, conventional image processing techniques do not consider these properties for their target images. So previous studies[4], [5] , which use conventional image processing techniques, sometime fail to obtain robust results of smoke detection by the effect of above properties of smoke in some cases.

In this study, we examine a smoke detection method which considers characteristic properties of smoke. That is, we assume that smoke is fractal[9], [10], [11].From this assumption, we can characterize the fractal nature of smoke with the *Hurst exponent*(H), which is a widely known and used fractal exponent. H is defined on two-dimensional regions of images and it takes unique value for each fractal–type. So we can characterize the fractal regions in given images with H. We firstly extract moving objects or areas as candidates of smoke regions. From these candidates, we classify smoke regions using H. To obtain H of a region in the image, we use *Averaged Wavelet Coefficient* (AWC) method[12], [13]. AWC method estimates the values H of the regions in images from the relation between H and the wavelet coefficient of the region. Using the estimated value of H, we discriminate whether the region is a smoke area or not. To obtain more accurate results of smoke detection, we also accumulate the results of discrimination based H about time. To evaluate the performance of this method, we use the real outdoor scenes obtained from the fixed single camera. Under some thresholding parameters settings, we examine the smoke detection results and show the effectiveness of this method.

II. Pre–processing

We consider smoke is the moving object in the image sequence. Extracted regions as moving objects are candidates of smoke regions. As pre–processing, we detect moving objects in the image sequence as candidates of smoke regions in pre–processing. We use 30 frame–per–second rate image sequences, $f(t)$ ($t = 0, 1, 2, \cdots$(frame)) (Fig. 1(a)), as input image sequences in the following processing. We extract regions of moving objects with the image subtraction technique. As a growth–speed of smoke is considered, we subtract original

978-1-4244-6392-3/10/$26.00 ©2010 IEEE

image sequence at one second intervals and obtain subtract images at every 5 frame of $f(t)$. In this case, this threshold value (5 frame) is selected manually. So the subtracted image frame $g(t)$ is written as $g(t) = |f(t) - f(t-30)|$ $(t = 30, 35, 40, \cdots$(frame)) (Fig. 1(b)).

(a) Original image (b) Subtracted image

Fig. 1. An example image of the pre–processing (subtraction) result.

III. Principles of smoke detection

A. Fractal property of smoke

We can observe many examples of fractal in natural images, for example, landscapes[6], plants[7] and clouds[8]. These are considered and modeled as stochastic processes. As smoke is also considered as Brownian motion, one of the popular stochastic process, at the molecular level, it is natural we assume that smoke is fractal. Moreover, we assume smoke is *self-affine-fractal*($\mathcal{SAF}$)[14]. From this assumption, smoke has some features of fractal and hence it is characterized with some index numbers. In this study, we focus on the Hurst exponent H to measure the property of $\mathcal{SAF}$ of smoke. Using this H, we determine smoke areas in the image. Note that we also assume that the subtracted image $g(t)$ is $\mathcal{SAF}$. After the pre–processing described above, we use $\mathcal{SAF}$ property of the subtracted image $g(t)$ in our method.

The assumption of $\mathcal{SAF}$ on smoke described above provides us how to determine which regions in the image. That is, we can use the Hurst exponent H in the smoke detection. Here we describe the definition of H and how to use it in our method.

B. $\mathcal{SAF}$ and Hurst Exponent

If an image $h(x, y)$ is $\mathcal{SAF}$, $h(x, y)$ satisfies the following relation under the transformation $(x, y) \rightarrow (\lambda x, \lambda y)$:

$$h(x, y) \simeq \lambda^{-H} h(\lambda x, \lambda y) \tag{1}$$

where H is called Hurst exponent. That is, $h(x, y)$ is controlled by the scaling parameter λ and H. From the relation (1), we obtain the characteristic value H which reflects the $\mathcal{SAF}$ property of $h(x, y)$

C. Relation between Hurst Exponent and Wavelet Coefficient

To calculate H of the image $h(x, y)$, we use the relation between the wavelet coefficient [15] of $h(x, y)$ and H as follows[12][13] :

$$\begin{aligned} &W\{h(x, y), a, b_x, b_y\} \\ &\quad = \frac{1}{a} \int\int \psi^* \left(\frac{x - b_x}{a}, \frac{y - b_y}{a} \right) h(x, y) dx dy \end{aligned} \tag{2}$$

$$W\{h(x, y), a, x, y\} \propto a^{H+1} \tag{3}$$

where ψ is the mother or analyzing wavelet that has the *scale parameter* a and the *translation parameter* b. From the relation (3), we obtain H of $h(x, y)$ by changing a of the wavelet coefficient W.

D. Numerical calculation of Hurst exponent : Local Hurst exponent

When we treat real data, it is known that the numerically calculated H has fluctuation[12][1] To avoid this, we employ the averaging method AWC. In AWC, the wavelet coefficient value W at (x, y) is averaged out with its neighborhood's Ws. So AWC is mathematically defined as the following equation[13] :

$$\begin{aligned} &\overline{|W(h(x, y), a, x_0, y_0)|} \\ &\quad = \frac{1}{w^2} \sum_{x=x_0-(1/2)w, y=y_0-(1/2)w}^{x=x_0+(1/2)w, y=y_0+(1/2)w} |W(h(x, y), a, x, y)| \end{aligned} \tag{4}$$

where w is the parameter that define the size of the neighborhood at (x, y). From Eq. (4), we obtain the Hurst exponent without the numerical fluctuation. We call this *Local Hurst exponent* H_l. To calculate the H_l of each point in $g(t)$, we define the (Local) Hurst exponent of the point in the target rectangle as H_l. The detection process of smoke becomes the rectangle–based as for AWC. Fig. 2 shows the scan process with the rectangle window on $g(t)$. We scan whole of the image $g(t)$ with the rectangle window whose window size is w and calculate H_l of these rectangles. To avoid the computation complexity, we scan the image every 4 pixels horizontal and vertical directions and we set the value of H_l of every point in the same rectangle window to be that of the center point of the rectangle. Based on these H_l, we determine which rectangles are smoke.

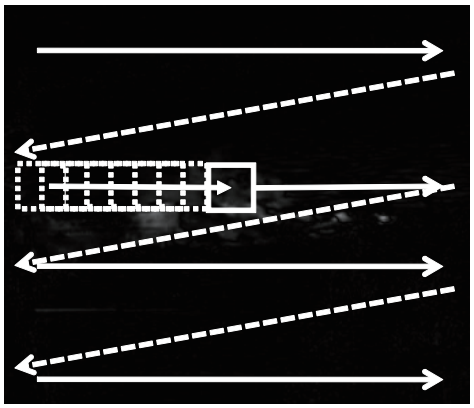

Fig. 2. Scanning with the rectangle window on $g(t)$ and the calculation of H_l on each rectangle.

[1]This fluctuation is caused from the numerical calculation of the wavelet coefficient.

E. Extraction of smoke regions using H_l

To extract smoke regions in images, we compare H_l of the target region(rectangle) with the H_l of *ideal smoke*, which is the set consists of preliminary prepared smoke regions. The ideal smoke set consists of manually selected rectangle regions of smoke, and the rectangle's size is $w \times w$ same as the window size in Eq. (4). We scan $g(t)$ with the rectangle window and calculate the value of H_l of each rectangle region. If the H_l of the target rectangle is similar to the H_l of the ideal smoke, we determine it is smoke. That is, we set the label of the target rectangle $l_g(x, y; t)$ to 1, else we set it to 0 as Eq. (5).

$$l_g(x, y; t) = \begin{cases} 1 \ ((x, y) \ is \ determined \ as \ smoke) \\ 0 \ (else) \end{cases} \quad (5)$$

where (x, y) is a point in the target rectangle.

F. Time Accumulation

To detect smoke in real scenes, we have sometime difficulties using only one index due to effects of several conditions. For example, there exist several kinds of non–smoke objects as noises. To remove the effect of these non–smoke objects, we consider the property of smoke as moving objects. That is, smoke almost appears the same place during the source of fire exist. Here we accumulate the results with H_l about *time* to realize this. The accumulation is defined as follows:

$$\mathcal{A}_g(x, y; t) = \sum_{t=\tau}^{\tau+T} l_g(x, y; t) \quad (6)$$

where $l_g(x, y; t)$ is the label of (x, y) described in Eq. (5) and accumulation time T is must be selected manually. Fig. 3 shows the time–accumulation process of the results with H_l described in III-E. This point-wise accumulation of the label

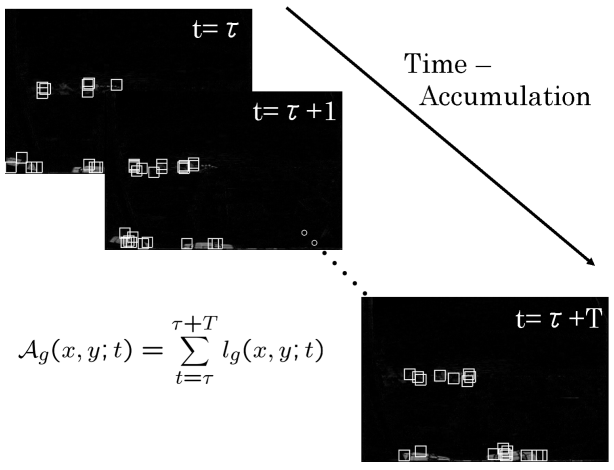

Fig. 3. Time accumulation of the results with H_l.

about time provides us the information which point is similar to smoke. That is, if $\mathcal{A}_g(x, y; t)$ takes high value, that point is similar to smoke. Based on $\mathcal{A}_g(x, y; t)$, we can do the point-wise extraction of smoke regions.

IV. Experiments using Real Scenes

To evaluate our method, we do experiments using image sequence obtained from a surveillance camera in the real scene. The size of this image sequences is $720 \times 480(px)$, and it contains smoke and other moving objects such as humans and cars. An example of the image is shown in Fig. 1 (a). In the following experiments, we set the window size w in Eq. (4) the fixed value, $32 \times 32(px)$, and the scanning window size of the rectangle (see III-E) is same.

As the ideal smoke set, we prepare the image set which consists of manually selected 171 $32 \times 32(px)$ rectangle regions of smoke.

A. Ideal smoke and its Hurst Exponent

We measure the similarity between the target region and the ideal smoke using H_l. To calculate H_l, we need to select the mother wavelet in Eq.(2). Since all distributions using several different mother wavelets have sharply-peaked shapes. So the selection of the mother wavelet does not affect to measure the similarity[16]. This support that smoke is fractal, that is our assumption.

In the following experiment, we use *Coiflet* as the mother wavelet.

B. Discrimination of smoke regions based on H_l

We discriminate the smoke regions in $g(t)$ using H_l of ideal smoke. Firstly, we scan the $g(t)$ with the rectangle window and calculate the H_l of that target rectangle. If H_l of the target rectangle is in *mean* $\pm$ *variance* of the ideal smoke, we discriminate the target rectangle as the smoke area. In this case, H_l's range of smoke is 0.670041 ± 0.004676. Examples of the results are shown in Fig. 4 and Fig. 5 respectively.

From these results, we can detect smoke and roughly extract the smoke regions. However, like the example in Fig. 5 , some moving objects are detected as failures. This is because some moving objects happen to have similar values of H_l compare to that of ideal smoke. Once the rectangle have the similar value, the rectangle are detected as smoke in many frames. To solve this problem, we consider to use the time accumulation of the results of H_l. This works well if the moving object does not have similar properties of smoke described above.

C. Comparison of discrimination results with time accumulation

To obtain the accurate result, we use the time accumulation technique (see. III-F) . The result of the accumulation is affected by the accumulation time T and the threshold value of $\mathcal{A}_g$ in Eq. (6). We evaluate the effect of these parameters' settings.

In first example, we choose the cases of $T = 15$, 20 and 25, and we select the threshold values of $\mathcal{A}_g$ to be 60% and 80% of T, respectively. Figure 6 shows example images in the case of $T = 15$, $T = 20$ and $T = 25$ and the threshold value is 60% of T, and Figure 7 shows example images in the case of $T = 15$, $T = 20$ and $T = 25$ and the threshold value is 80% of T, respectively.

(a) Original image

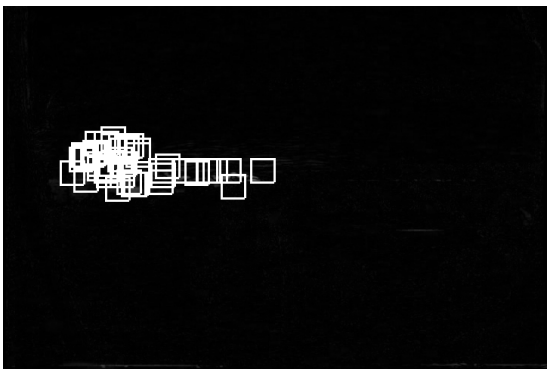

(b) Detection result with H_l

Fig. 4. An example image of smoke detection with H_l.

(a) Original image

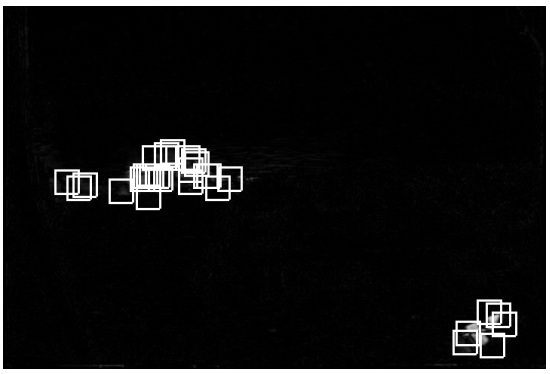

(b) Detection result with H_l

Fig. 5. An example image of smoke detection with H_l (including failure detections).

In both cases, we use the same original image. From these results, we can observe that when in cases of (i) $T = 15, 20$, the threshold is 60%, and (ii)$T = 15$, the threshold is 80%, there remains the failure detection at the bottom of the right side of the image sequence. However, when in cases of $T = 25$ the threshold value is 80%, the extracted area of smoke is too small compared to the original image. So the most accurate result is in the case of $T = 25$ and threshold 60% and $T = 20$ and threshold 80% in this experiment.

Figure 8 shows another example of the experiments. In this case, we choose the cases of $T = 15$, 20 and 25,a and we select the threshold value to be 60% of T. And the location is also same but the wind condition is different from the example of Figs. 6 and 7. Because the wind is weak, the smoke region is small and the change of luminance is also small. Even in the different conditions, our method can detect the smoke area. This result also shows that the difference of T does not affect the result of extraction of smoke areas. So the optimal parameter is $T = 15$ because the time–delay is minimum in this example.

From these results, we confirm that our method can detect the smoke area under suitable parameters.

There remains some problems for the further study. The accumulation length of time affects the positional misalignment of the smoke areas and the time delay. On the other hand, threshold value affects the accuracy of the detection of the smoke. As a result, these two parameters relatively affects the accurate detection and extraction result each other. To construct more realistic system, we need the further study of the optimal and automatic selection method of these parameters.

V. Conclusions and Further works

In this study, we study the method of the smoke detection based on the characteristic property of smoke as fractal. As the characteristic of fractal nature of smoke, we use the Hurst exponent H defined by the relation between H and the Wavelet coefficient. To determine which regions of images are smoke, we use H of each regions. We employ the averaging method, AWC, to avoid the numerical fluctuation of H.

In our method, moving objects in images are extracted as the candidate regions of smoke. Instead of ideally defined H, we use the local Hurst exponent H_l, the averaged value of H calculated with AWC, to determine whether these candidate regions are smoke or not. Moreover, to obtain more accurate results of the detection, we accumulate the result of detection in each image about time. The time–accumulation works well, as smoke has different properties from other moving objects which even has the similar value of H compared to smoke's one.

To evaluate our method, we examine it with some examples of image sequences. In the example images, there exist smoke and other moving objects which are considered as obstructions.

(a) Original image

(b) T=15 (threshold :9)

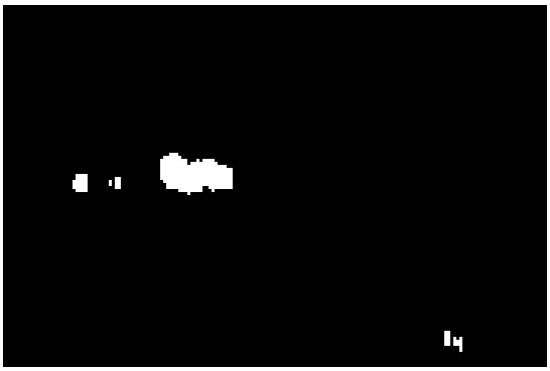

(c) T=20 (threshold :12)

(d) T=25 (threshold :15)

Fig. 6. Smoke detection of time accumulation for each T. The threshold value is set to be 60% of T.

(a) Original image

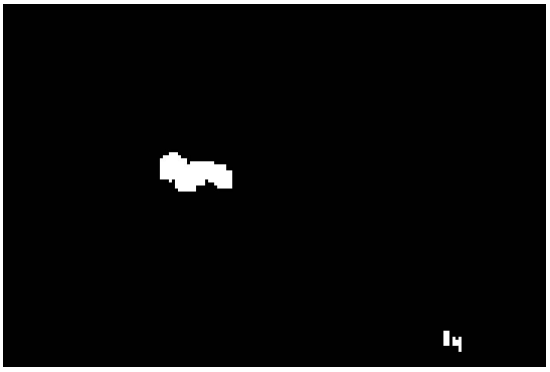

(b) T=15 (threshold :12)

(c) T=20 (threshold :16)

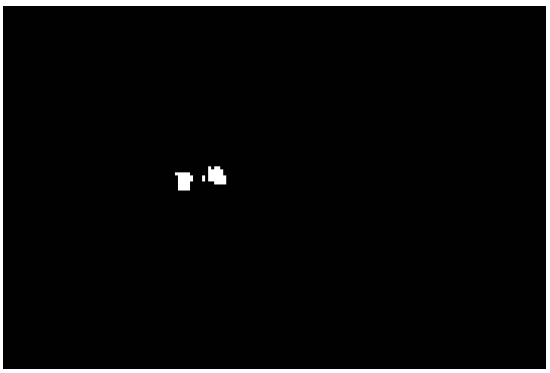

(d) T=25 (threshold :20)

Fig. 7. Smoke detection of time accumulation for each T. The threshold value is set to be 80% of T.

(a) Original image

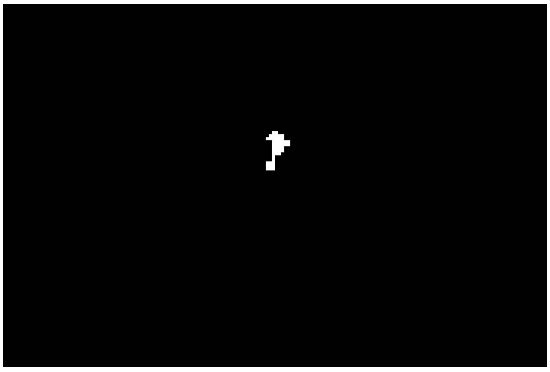

(b) T=15 (threshold :9)

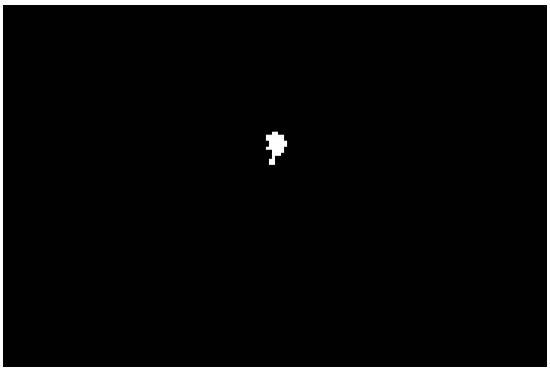

(c) T=20 (threshold :12)

(d) T=25 (threshold :15)

Fig. 8. Another result of smoke detection of time accumulation for each T. The threshold value is set to be 60% of T.

Experimental results show the effectiveness of our method. However, the experiment also show some parameters which are manually selected affect the result. So we need the further research to select these parameter optimally and automatically.

There remain some problems for further works. One is that we need a more accurate estimation of the smoke region. To obtain the accurate regions of smoke in the images, it is useful to use the statistical distribution of the *ideal smoke* set. Additionally, it is needed to evaluate using more data obtained in different conditions such as lighting, complex backgrounds, and moving objects of varied categories and sizes. We also plan to use other fractal indexes of stochastic processes and combine these indexes for the good performance.

ACKNOWLEDGMENT

This work is supported in part by the Grant-in-Aid for Scientific Research (No. 21360134) of JSPS (Japan Society for the Promotion of Science) and the Ministry of Education, Science, Sports and Culture.

REFERENCES

[1] W. Phillips III, M. Shah and N. V. Lobo: "Flame recognition in video," Pattern Recognition Lett., 23, pp. 319–327, 2002.
[2] C. B. Liu and N. Ahuja: "Vision based fire detection," Proc. of the International Conference on Pattern Recognition, Vol. 4, pp. 134–137, 2004.
[3] B. U. Töreyin, Y. Dedeoglu, U. Güdükday and A. E. Qetin: "Computer vision based method for real–time fire and flame detection," Pattern Recognition Lett., 27, pp. 49–58, 2006.
[4] B. U. Töreyin, Y. Dedeoglu and A. E. Enis: "Wavelet based real–time smoke detection in video," Proc. of the European Signal Processing Conference, 2005.
[5] B. U. Töreyin, Y. Dedeoglu and A. E. Enis: "Contour based smoke detection in video using wavelet," Proc. of the European Signal Processing Conference, 2006.
[6] C. M. Hagerhall, T. Purcella and R. Taylor: "Fractal dimension of landscape silhouette outlines as a predictor of landscape preference," Journal of Environmental Psychology, Vol. 24, pp. 247–255, 2004.
[7] O. M. Bruno, R. de Oliveira Plotze, M. Falvo and M. de Castro: "Fractal dimension applied to plant identification," Information Sciences, Vol. 178, pp. 2722–2733, 2008.
[8] R. F. Cahalan and J. H. Joseph: "Fractal Statistics of Cloud Fields," Monthly Weather Review, Vol. 117, pp. 261–272, 1989.
[9] B. Mandelbrot: "The Fractal Geometry of Nature," Freeman and Company, 1982.
[10] M. Barnsley: "Fractals Everywhere," 2nd ed., Academic Press, 1993.
[11] H. Peitgen, H. Jürgens, D. Saupe: "Fractals for the Classroom: Part 1: Introduction to Fractals and Chaos," Springer-Verlag, 1992.
[12] I. Simonsen, A. Hansen and O. M. Nes: "Determination of the Hurst Exponent by use of Wavelet Transforms," Phys. Rev., B, No.58, pp. 2779–2787, 1998.
[13] K. Yamagiwa, M. Takanashi, S. Izumi and S. Sakai: "Method for Characterizing Fracture Surface by Using Two–Dimensional Local Hurst Exponent, and its Application to the Quantitative Evaluation of Stretched–Zone Width," Trans. of the Japan Society of Mechanical Engineers, Series A, Vol. 71, No. 705, pp. 749–754, 2005 (in Japanese).
[14] B. Mandelbrot: "Self–Affine Fractals and Fractal Dimension," Physica Script, Vol. 32, pp. 257–260, 1985.
[15] C. Chui: "An Introduction to Wavelets," Academic Press, 1992.
[16] H. Maruta, T. Yamamichi and Fujio Kurokawa: "A New smoke detection method based on local hurst exponent," Proc. of International Workshop Advanced Image Technology, 2010.